Supplementary Material

Figure S1

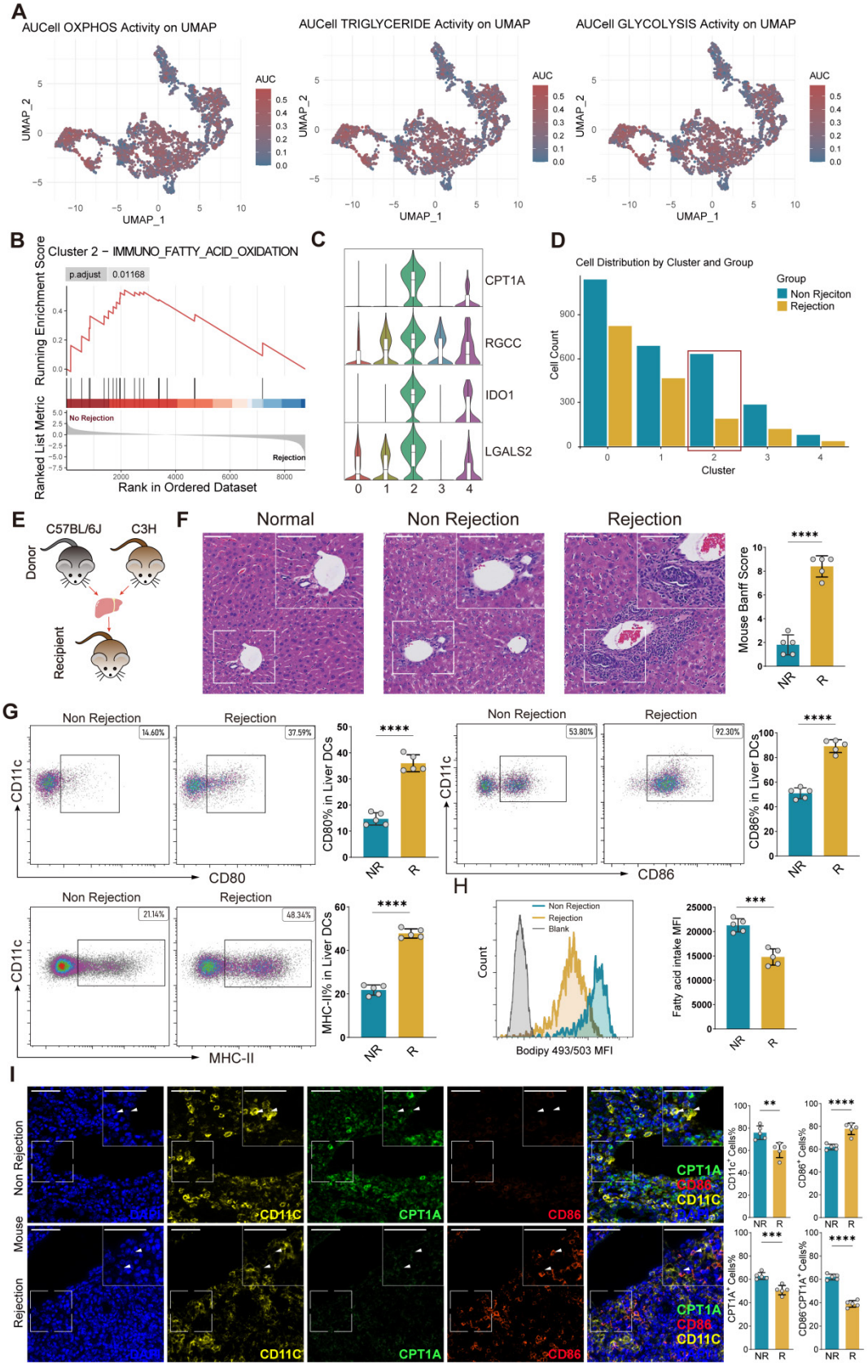


Figure S1. Metabolic heterogeneity of dendritic cell subsets and in situ analysis of CPT1A and CD86 expression in murine liver DCs.

(A) AUCell analysis of oxidative phosphorylation, triglyceride metabolism, and glycolytic activity across dendritic cell (DC) clusters. **(B)** Gene set enrichment analysis (GSEA) plot showing fatty acid oxidation (FAO) pathway enrichment in cluster 2 DCs from the non-rejection (NR) and rejection (R) groups. **(C)** Violin plots showing the expression of CPT1A, RGCC, IDO1, and LGALS2 across DC clusters. **(D)** Bar plot showing the cell distribution across DC clusters in the NR and R groups. (**E-F**) Schematic and H&E staining of murine liver transplantation models with Banff score quantification. Scale bars, 100 μm. **(G)** Flow cytometry analysis of CD80, CD86, and MHC-II expression in liver DCs from the murine NR and R groups. **(H)** BODIPY 493/503 staining showing fatty acid uptake in liver DCs from the murine NR and R groups. **(I)** Immunofluorescence staining and quantification of CD11c, CPT1A, and CD86 in liver grafts from the murine NR and R groups. Scale bars, 50 μm.

Figure S2

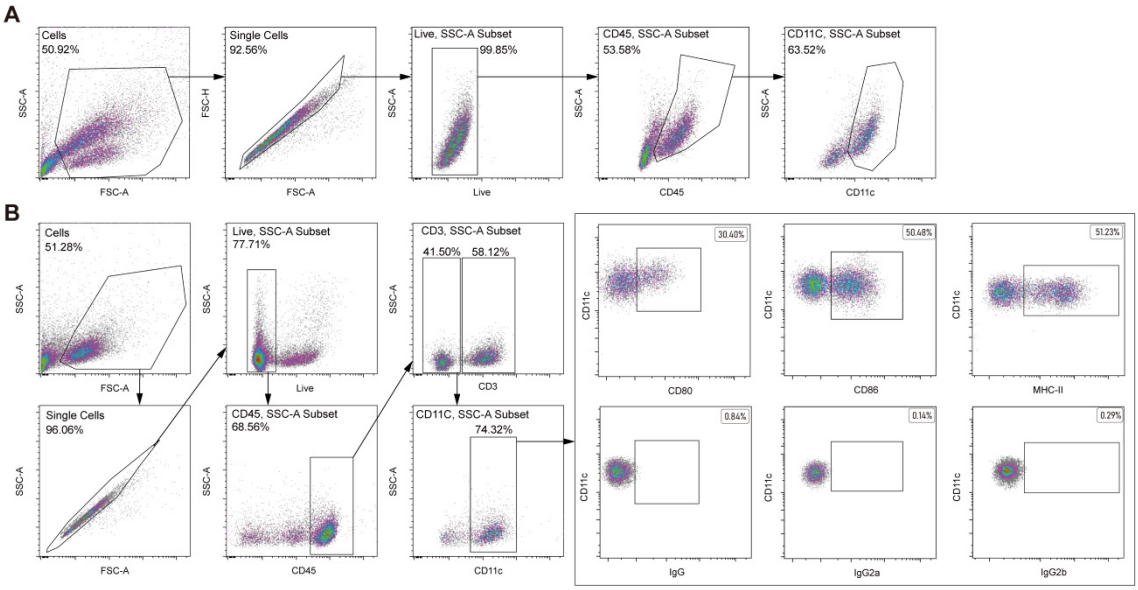


Figure S2. Flow cytometric gating strategies for dendritic cells in human PBMCs and murine liver, with representative isotype controls.

(A) Human peripheral blood mononuclear cells (PBMCs) were sequentially gated as total cells, singlets, live cells, $CD45^+$ leukocytes, and $CD45^+CD11c^+$ dendritic cells. **(B)** Murine hepatic mononuclear cells were sequentially gated as total cells, singlets, live cells, $CD45^+$ leukocytes, $CD3^-$ cells, and $CD45^+CD3^-CD11c^+$ dendritic cells. Representative staining for CD80, CD86, and MHC-II (upper panels) and the corresponding IgG1 isotype controls (lower panels) are shown.

Figure S3

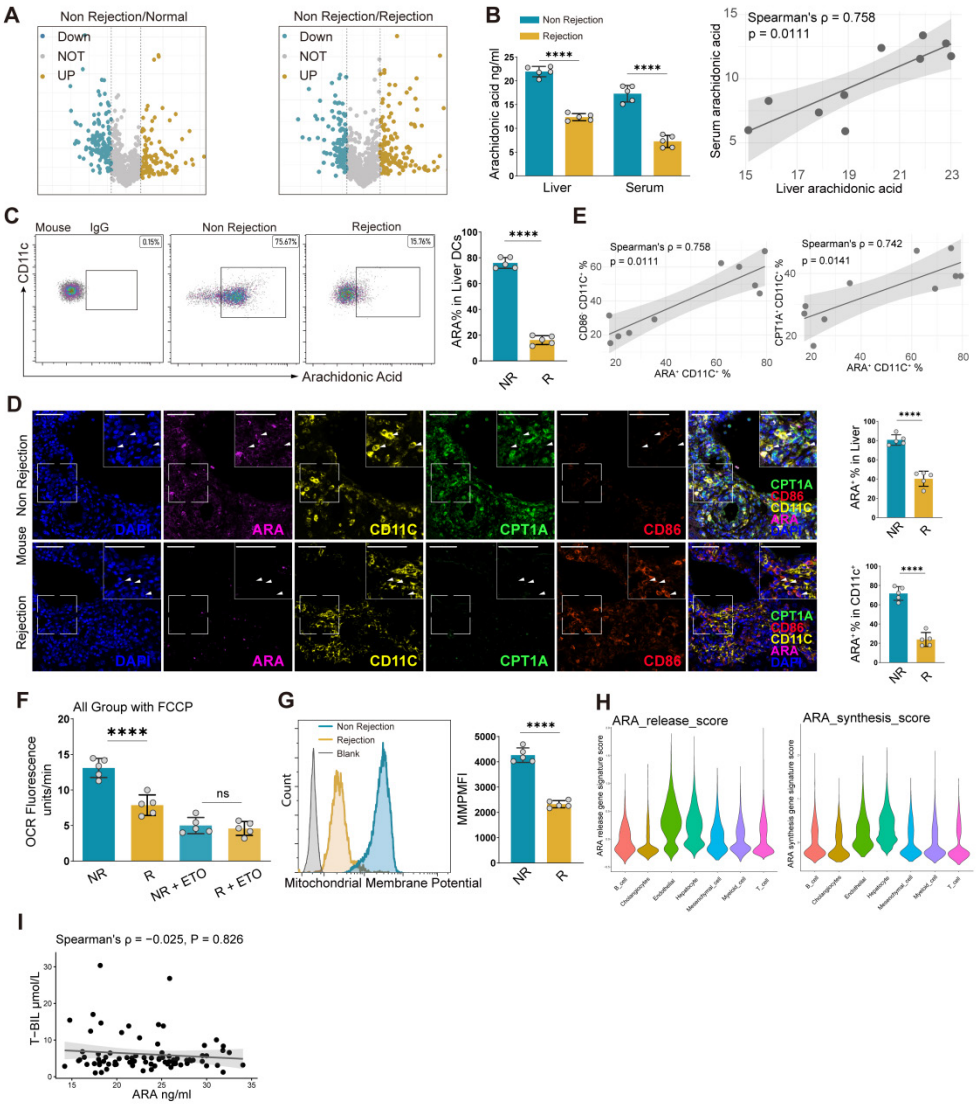

A
Non Rejection/Normal
Non Rejection/Rejection
Down
NOT
UP
B
Non Rejection
Rejection
Arachidonic acid ng/ml
Liver
Serum
Spearman's ρ = 0.758
p = 0.0111
Serum arachidonic acid
Liver arachidonic acid
C
Mouse IgG
Non Rejection
Rejection
CD11c
Arachidonic Acid
ARA% in Liver DCs
NR
R
E
Spearman's ρ = 0.758
p = 0.0111
Spearman's ρ = 0.742
p = 0.0141
CD86+ CD11C+ %
CPT1A+ CD11C+ %
ARA+ CD11C+ %
D
Non Rejection
Mouse
Rejection
DAPI
ARA
CD11C
CPT1A
CD86
ARA+ % in Liver
ARA+ % in CD11c+
F
All Group with FCCP
OCR Fluorescence units/min
NR
R
NR + ETO
R + ETO
ns
G
Non Rejection
Rejection
Blank
Count
Mitochondrial Membrane Potential
MMPMFI
H
ARA_release_score
ARA_synthesis_score
I
Spearman's ρ = −0.025, P = 0.826
T−BIL μmol/L
ARA ng/ml

Figure S3. Altered metabolic and functional features of liver dendritic cells in mouse liver transplantation.

(A) Volcano plots of metabolites in the non-rejection (NR) versus normal and NR versus rejection (R) groups. **(B)** Arachidonic acid (ARA) levels in murine liver and serum, with correlation analysis. **(C)** Flow cytometry analysis of ARA in liver dendritic cells (DCs) from the murine NR and R groups. **(D)** Immunofluorescence staining and quantification of ARA, CD11c, CPT1A, and CD86 in liver DCs from the murine NR and R groups. Scale bars, 50 μm. **(E)** Spearman correlation analysis of $ARA^{+}CD11c^{+}$ DCs with $CD86^{+}CD11c^{+}$ or $CPT1A^{+}CD11c^{+}$ DCs based on immunofluorescence staining in the murine groups. **(F)** Oxygen consumption rate in murine liver DCs from the NR and R groups with or without etomoxir treatment. **(G)** Mitochondrial membrane potential (MMP) analysis in murine liver DCs from the NR and R groups. **(H)** ARA release and synthesis scores across human liver cell types. **(I)** Spearman correlation analysis between serum ARA and T-Bil levels.

Figure S4

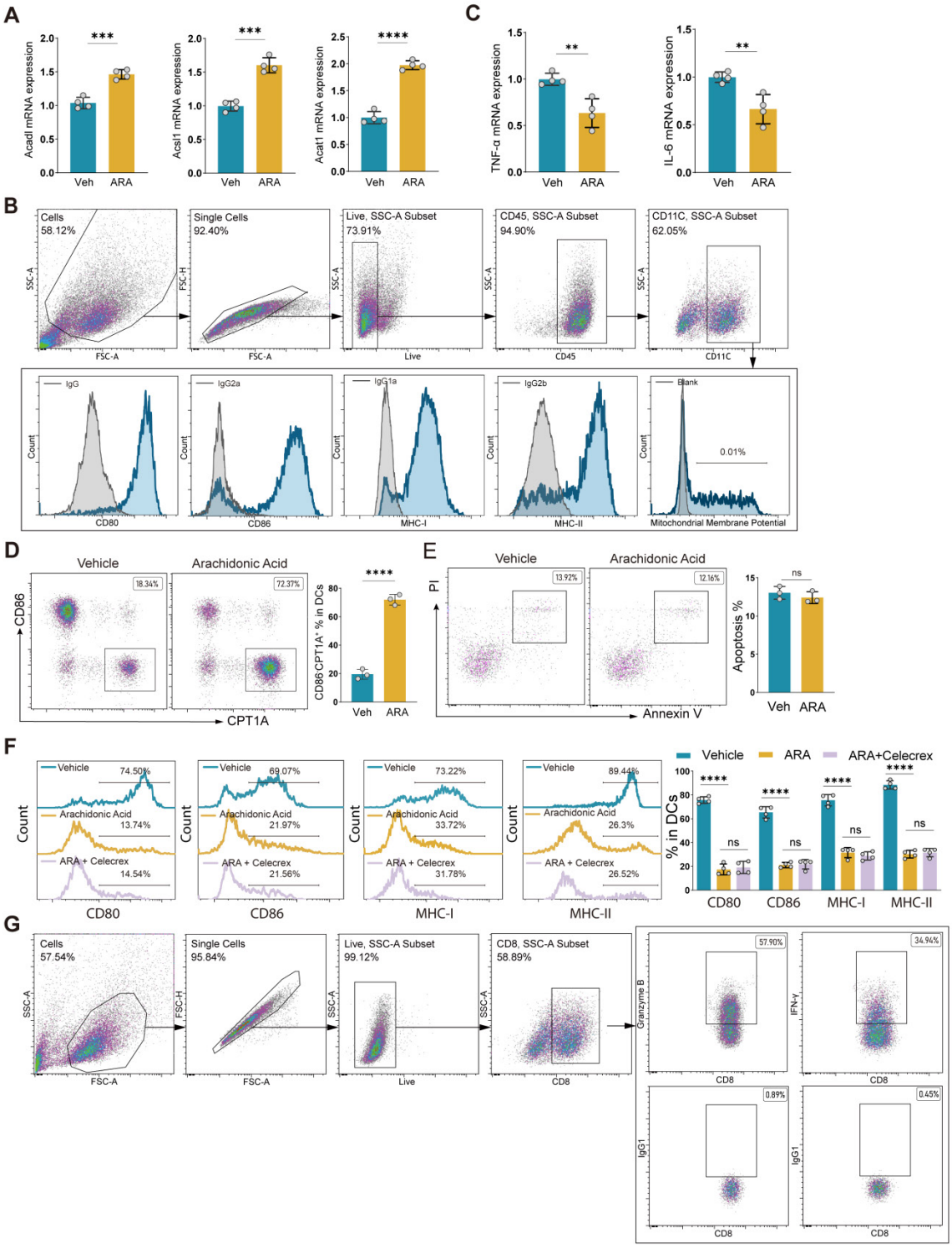

A
Acadl mRNA expression
Acsl1 mRNA expression
Acat1 mRNA expression
Veh
ARA
C
TNF-α mRNA expression
IL-6 mRNA expression
B
Cells
58.12%
Single Cells
92.40%
Live, SSC-A Subset
73.91%
CD45, SSC-A Subset
94.90%
CD11C, SSC-A Subset
62.05%
IgG
IgG2a
IgG1a
IgG2b
Blank
0.01%
CD80
CD86
MHC-I
MHC-II
Mitochondrial Membrane Potential
D
Vehicle
Arachidonic Acid
18.34%
72.37%
CD86
CPT1A
CD86 CPT1A+ % in DCs
E
13.92%
12.16%
PI
Annexin V
Apoptosis %
ns
F
Vehicle
Arachidonic Acid
ARA + Celecrex
74.50%
13.74%
14.54%
69.07%
21.97%
21.56%
73.22%
33.72%
31.78%
89.44%
26.3%
26.52%
Count
CD80
CD86
MHC-I
MHC-II
ARA
ARA+Celecrex
% in DCs
ns
G
Cells
57.54%
Single Cells
95.84%
Live, SSC-A Subset
99.12%
CD8, SSC-A Subset
58.89%
Granzyme B
IFN-γ
IgG1
57.90%
34.94%
0.89%
0.45%
CD8

Figure S4. Arachidonic acid-induced tolerogenic reprogramming of dendritic cells is independent of apoptosis and COX-PGE2 signaling, and CD86$^-$CPT1A^high DCs suppress CD8$^+$ T-cell responses in co-culture.

(A) mRNA expression of Acadl, Acsl1, and Acat1 in bone marrow derived dendritic cells (BMDCs) treated with vehicle (Veh) or arachidonic acid (ARA). **(B)** Representative gating strategy for CD80, CD86, MHC-I, and MHC-II expression in CD45$^+$CD11c$^+$ DCs. **(C)** mRNA expression of TNF-α and IL-6 in BMDCs in the Veh and ARA groups. **(D)** Representative flow cytometry plots and quantification of CD86-CPT1A$^+$ cells among vehicle or ARA groups. **(E)** Flow cytometry analysis of apoptosis in BMDCs in the Veh or ARA groups. **(F)** Flow cytometry analysis of CD80, CD86, MHC-I, and MHC-II expression in BMDCs in the Veh, ARA, or ARA + celecoxib groups. **(G)** Representative gating strategy for determining granzyme B and IFN-γ expression in CD8$^+$ T cells.

Figure S5

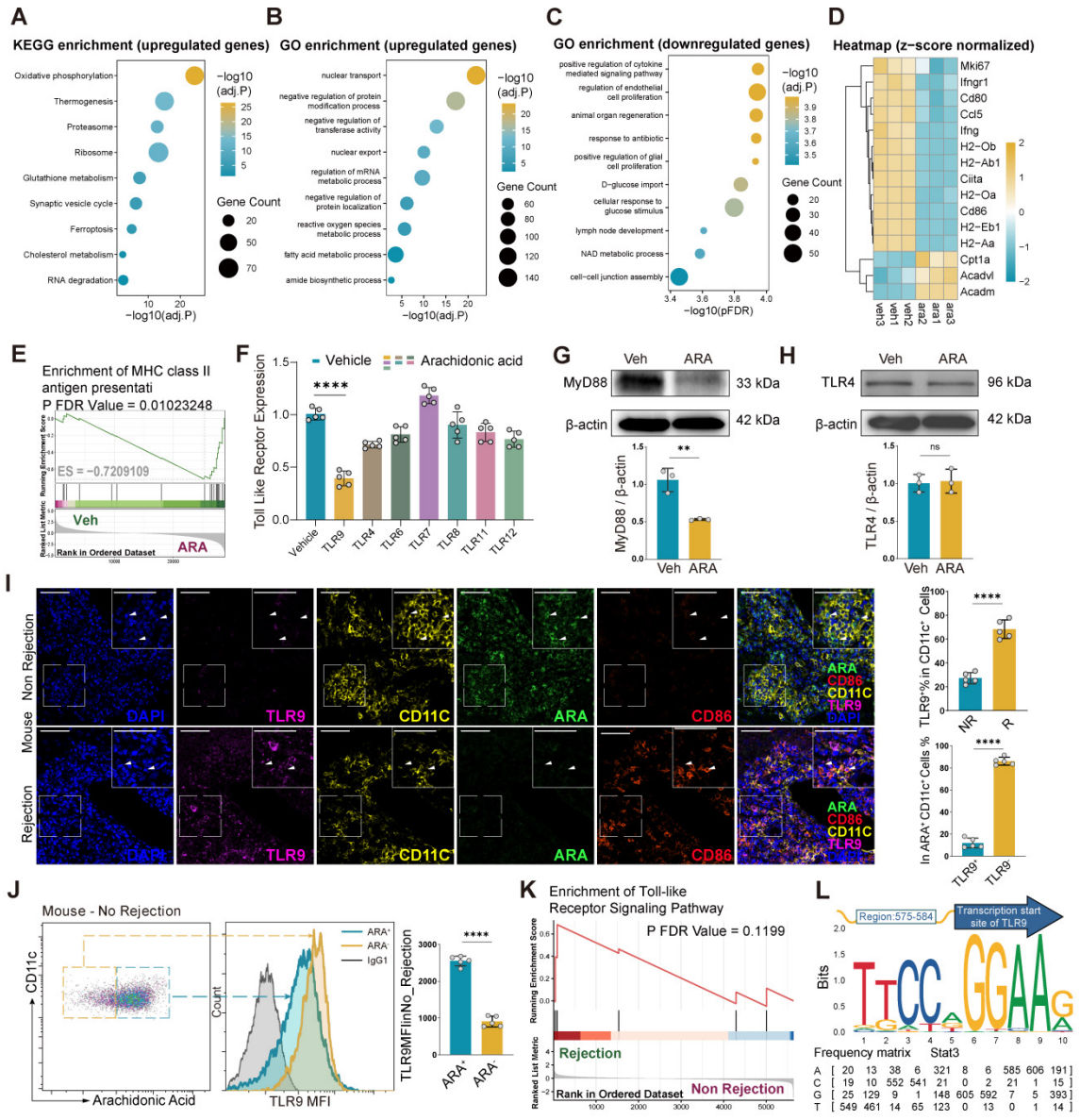

A
KEGG enrichment (upregulated genes)
Oxidative phosphorylation
Thermogenesis
Proteasome
Ribosome
Glutathione metabolism
Synaptic vesicle cycle
Ferroptosis
Cholesterol metabolism
RNA degradation
−log10(adj.P)
Gene Count
B
GO enrichment (upregulated genes)
nuclear transport
negative regulation of protein modification process
negative regulation of transferase activity
nuclear export
regulation of mRNA metabolic process
negative regulation of protein localization
reactive oxygen species metabolic process
fatty acid metabolic process
amide biosynthetic process
C
GO enrichment (downregulated genes)
positive regulation of cytokine mediated signaling pathway
regulation of endothelial cell proliferation
animal organ regeneration
response to antibiotic
positive regulation of glial cell proliferation
D-glucose import
cellular response to glucose stimulus
lymph node development
NAD metabolic process
cell−cell junction assembly
−log10(pFDR)
D
Heatmap (z−score normalized)
Mki67
Ifngr1
Cd80
Ccl5
Ifng
H2−Ob
H2−Ab1
Ciita
H2−Oa
Cd86
H2−Eb1
H2−Aa
Cpt1a
Acadvl
Acadm
veh3
veh1
veh2
ara2
ara1
ara3
E
Enrichment of MHC class II antigen presentati
P FDR Value = 0.01023248
ES = −0.7209109
Veh
ARA
Rank in Ordered Dataset
F
Vehicle
Arachidonic acid
Toll Like Recptor Expression
****
Vehicle
TLR9
TLR4
TLR6
TLR7
TLR8
TLR11
TLR12
G
Veh
ARA
MyD88
33 kDa
β-actin
42 kDa
MyD88 / β-actin
**
H
Veh
ARA
TLR4
96 kDa
β-actin
42 kDa
TLR4 / β-actin
ns
I
Non Rejection
Rejection
Mouse
DAPI
TLR9
CD11C
ARA
CD86
TLR9+% in CD11c+ Cells
In ARA+ CD11c+ Cells %
NR
R
J
Mouse - No Rejection
CD11c
Arachidonic Acid
Count
TLR9 MFI
ARA+
ARA-
IgG1
TLR9MFIinNo_Rejection
K
Enrichment of Toll-like Receptor Signaling Pathway
P FDR Value = 0.1199
Rejection
Non Rejection
Rank in Ordered Dataset
L
Region:575-584
Transcription start site of TLR9
Bits
Frequency matrix
Stat3
A [20 13 38 6 321 8 6 585 606 191]
C [19 10 552 541 21 0 2 21 1 15]
G [25 129 9 1 148 605 592 7 5 393]
T [549 461 14 65 123 0 13 0 1 14]

Figure S5. Transcriptomic and in situ validation of suppressed TLR9 signaling in ARA-high dendritic cells.

(A) KEGG enrichment analysis of upregulated genes in bone marrow derived dendritic cells (BMDCs) in the vehicle (Veh) or arachidonic acid (ARA) groups. **(B)** GO enrichment analysis of genes upregulated in BMDCs in the Veh or ARA groups. **(C)** GO enrichment analysis of genes downregulated in BMDCs in the Veh or ARA groups. **(D)** Heatmap of the normalized expression of selected genes in BMDCs in the Veh- or ARA-treated groups according to the z-score. **(E)** GSEA plot showing enrichment of the MHC class II antigen presentation pathway in BMDCs in the Veh or ARA groups. **(F)** mRNA expression of Toll-like receptor genes (Tlr1-Tlr12) in BMDCs in the Veh and ARA groups. **(G)** Western blot analysis of MyD88 protein expression in BMDCs from the Veh or ARA groups. **(H)** Western blot analysis of the TLR4 protein in BMDCs in the Veh or ARA groups. **(I)** Multiplex immunofluorescence staining of TLR9, CD11c, ARA, and CD86 in murine non-rejection (NR) and rejection (R) group liver allografts. **(J)** Flow cytometry analysis of TLR9 expression in ARA^+ and ARA^- liver dendritic cells (DCs) from the murine NR group. Scale bars, 50 μm. **(K)** GSEA plot of the Toll-like receptor signaling pathway in the murine NR and R groups. **(L)** Predicted STAT3 binding site in the TLR9 promoter.

Figure S6

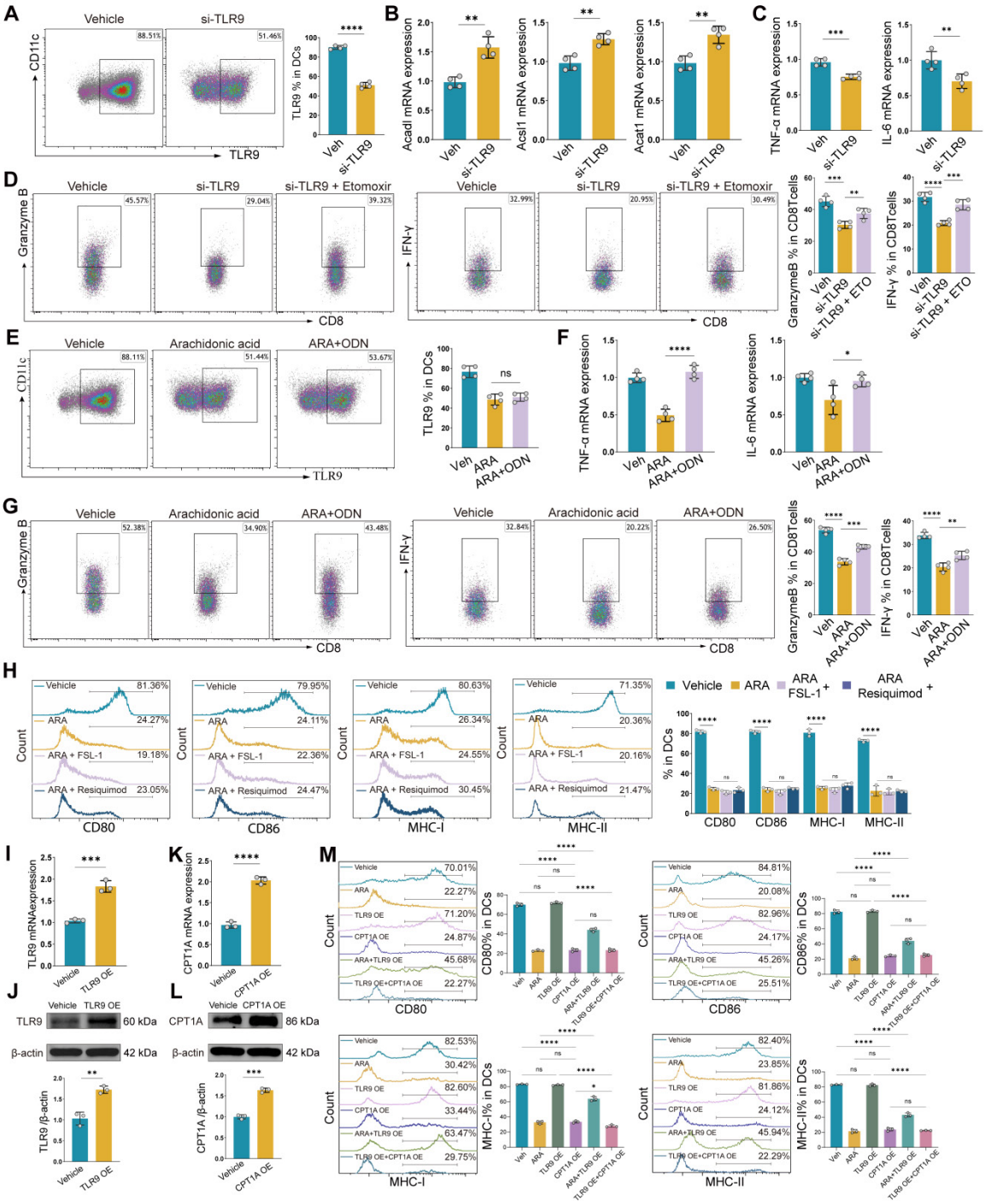

A
Vehicle
si-TLR9
CD11c
TLR9
88.51%
51.46%
TLR9 % in DCs
Veh
si-TLR9
B
Acadl mRNA expression
Acsl1 mRNA expression
Acat1 mRNA expression
C
TNF-α mRNA expression
IL-6 mRNA expression
D
Vehicle
si-TLR9
si-TLR9 + Etomoxir
Granzyme B
IFN-γ
CD8
45.57%
29.04%
39.32%
32.99%
20.95%
30.49%
GranzymeB % in CD8Tcells
IFN-γ % in CD8Tcells
si-TLR9 + ETO
E
Arachidonic acid
ARA+ODN
88.11%
51.44%
53.67%
ns
ARA
F
G
52.38%
34.90%
43.48%
32.84%
20.22%
26.50%
H
Count
ARA + FSL-1
ARA + Resiquimod
81.36%
24.27%
19.18%
23.05%
79.95%
24.11%
22.36%
24.47%
80.63%
26.34%
24.55%
30.45%
71.35%
20.36%
20.16%
21.47%
CD80
CD86
MHC-I
MHC-II
% in DCs
I
TLR9 mRNAexpression
Vehicle
TLR9 OE
J
TLR9
β-actin
60 kDa
42 kDa
TLR9 /β-actin
K
CPT1A mRNA expression
CPT1A OE
L
CPT1A
86 kDa
CPT1A /β-actin
M
70.01%
22.27%
71.20%
24.87%
45.68%
22.27%
84.81%
20.08%
82.96%
24.17%
45.26%
25.51%
CD80% in DCs
CD86% in DCs
82.53%
30.42%
82.60%
33.44%
63.47%
29.75%
82.40%
23.85%
81.86%
24.12%
45.94%
22.29%
MHC-I% in DCs
MHC-II% in DCs

Figure S6. Validation of the TLR9-dependent control of dendritic cell metabolic and immunoregulatory functions.

(A) Flow cytometry analysis of TLR9 expression in BMDCs in the vehicle (Veh) or si-TLR9 groups. **(B)** mRNA expression of Acadl, Acsl1, and Acat1 in bone marrow derived dendritic cells (BMDCs) treated with Veh or si-TLR9. **(C)** mRNA expression of TNF-α and IL-6 in BMDCs in the Veh or si-TLR9 groups. **(D)** Flow cytometry analysis of Granzyme B and IFN-γ in $CD8^+$ T cells co-cultured with BMDCs treated with Veh, si-TLR9, or si-TLR9 + ETO. **(E)** Flow cytometry analysis of TLR9 expression in BMDCs in the Veh, arachidonic acid (ARA), or ARA + ODN groups. **(F)** mRNA expression of TNF-α and IL-6 in BMDCs in the Veh, ARA, or ARA + ODN groups. **(G)** Flow cytometry analysis of Granzyme B and IFN-γ in $CD8^+$ T cells co-cultured with BMDCs treated with Veh, ARA, or ARA + ODN. **(H)** Flow cytometry of DC markers following ARA, FSL-1, or resiquimod treatment. **(I-J)** Verification of TLR9 overexpression (TLR9 OE) by RT-qPCR and western blotting. **(K-L)** Verification of CPT1A overexpression (CPT1A OE) by RT-qPCR and western blotting. **(M)** DC marker expression following Veh, ARA, TLR9 OE, CPT1A OE, ARA + TLR9 OE, TLR9 OE + CPT1A OE groups.

Figure S7

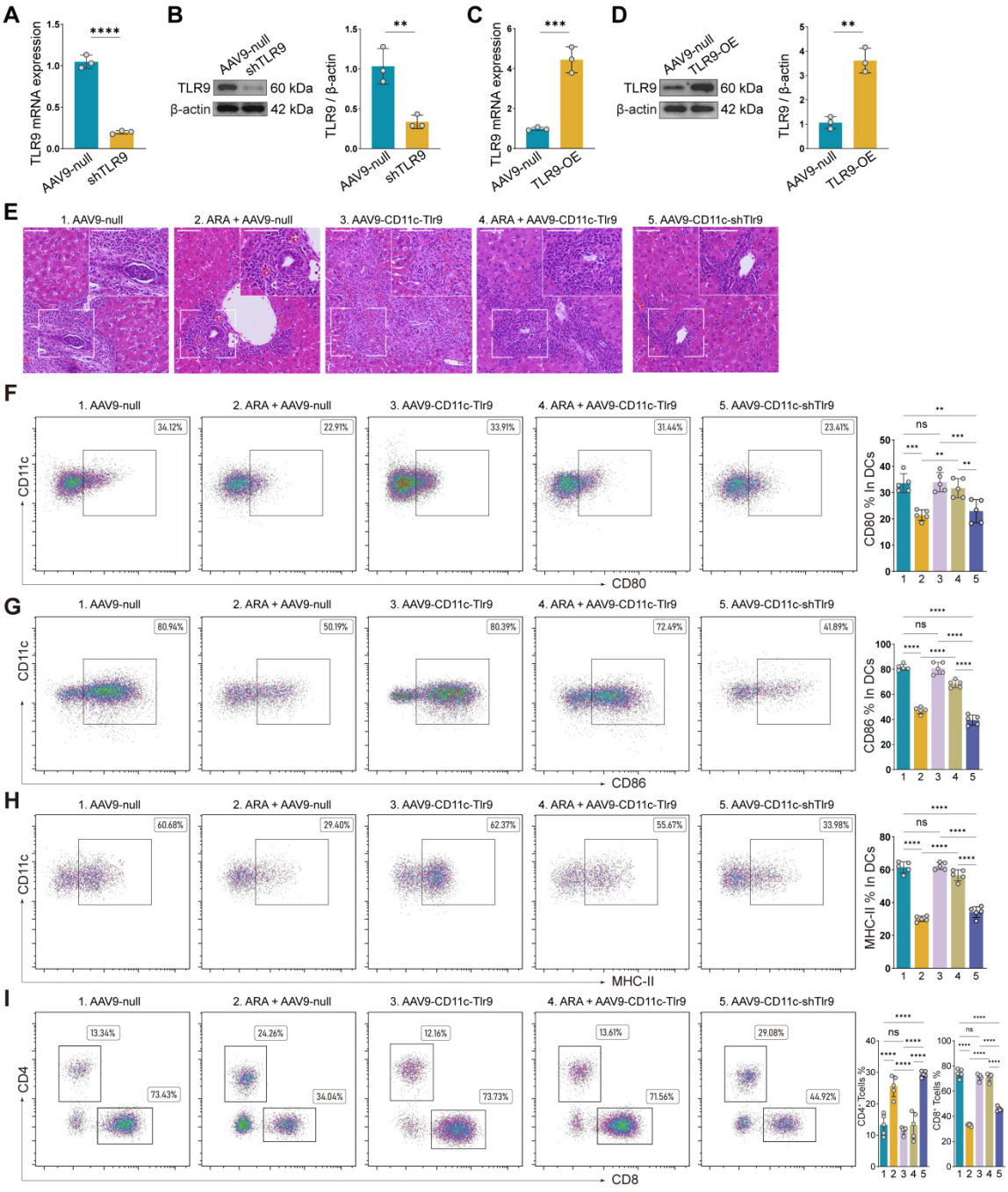

A
TLR9 mRNA expression
AAV9-null
shTLR9
B
AAV9-null
shTLR9
TLR9
60 kDa
β-actin
42 kDa
TLR9 / β-actin
C
TLR9 mRNA expression
AAV9-null
TLR9-OE
D
AAV9-null
TLR9-OE
TLR9
60 kDa
β-actin
42 kDa
TLR9 / β-actin
E
1. AAV9-null
2. ARA + AAV9-null
3. AAV9-CD11c-Tlr9
4. ARA + AAV9-CD11c-Tlr9
5. AAV9-CD11c-shTlr9
F
CD11c
CD80
CD80 % In DCs
G
CD11c
CD86
CD86 % In DCs
H
CD11c
MHC-II
MHC-II % In DCs
I
CD4
CD8
CD4+ Tcells %
CD8+ Tcells %

Figure S7. ARA suppresses hepatic DC activation and T-cell infiltration through TLR9 downregulation in liver allografts.

(A-B) qRT-PCR and Western blot analyses of TLR9 expression in murine hepatic DCs following AAV9-mediated TLR9 knockdown, with quantification of TLR9 protein levels. **(C-D)** qRT-PCR and Western blot analyses of TLR9 expression in murine hepatic DCs following AAV9-mediated TLR9 overexpression, with quantification of TLR9 protein levels. **(E)** Representative H&E staining of liver grafts from the AAV9-null, ARA + AAV9-null, AAV9-CD11c-TLR9, ARA + AAV9-CD11C-TLR9 and AAV9-CD11C-shTLR9 groups. Scale bars, 100 μm. **(F-H)** Flow cytometry analysis of CD80, CD86, and MHC-II expression in hepatic DCs from the indicated groups, with quantification of positive cell percentages. **(I)** Flow cytometry analysis of hepatic $CD4^+$ and $CD8^+$ T cells from the indicated groups, with quantification of cell percentages.

Figure S8

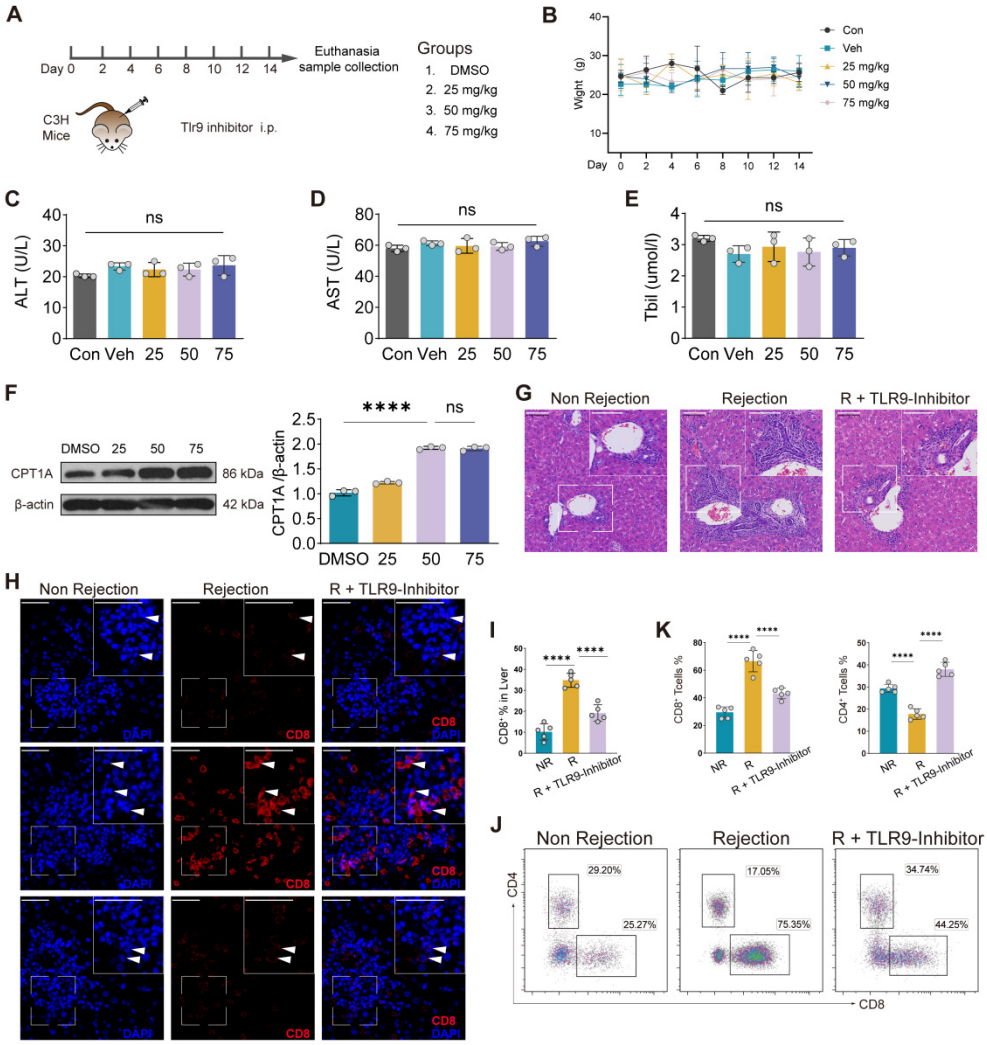


Figure S8. Safety evaluation of HCQ and analysis of graft-infiltrating T cells.

(A) Experimental scheme for intraperitoneal HCQ administration (25, 50, or 75 mg/kg) to C3H mice. **(B)** Body weight during the 14-day treatment period. **(C-E)** Serum ALT, AST, and T-BIL levels. **(F)** Western blot and quantification of CPT1A in hepatic DCs. **(G)** Representative H&E-stained liver allograft sections. Scale bar, 100 μm. **(H-I)** Representative immunofluorescence staining and quantification of intrahepatic $CD8^+$ cells. Scale bar, 50 μm. **(J-K)** Representative flow cytometry plots and quantification of intrahepatic $CD4^+$ and $CD8^+$ T cells. NR, non-rejection; R, rejection. Scale bars, 50 μm.

Inclusion and exclusion criteria

Liver transplant recipients were eligible for inclusion if they met all of the following criteria: (1) aged 18-65 years; (2) at least 6 months had elapsed since liver transplantation; and (3) they were able to understand the study procedures and voluntarily provided written informed consent.

Patients were excluded if they met any of the following criteria: (1) underwent ABO-incompatible liver transplantation; (2) received combined liver and other organ transplantation; (3) underwent liver retransplantation; (4) received pretransplant antitumor treatment, including systemic chemotherapy, hepatic arterial infusion chemotherapy, or transarterial chemoembolization; (5) developed a fungal infection or severe bacterial infection after transplantation; (6) developed severe postoperative vascular or biliary complications; (7) had suspected or confirmed graft-versus-host disease; or (8) were unable to fully understand the study procedures or provide written informed consent because of their health status, cognitive impairment, or other relevant conditions.

Withdrawal and discontinuation criteria

Participants were withdrawn from the study if they were subsequently found to have been incorrectly enrolled because they did not meet the inclusion criteria or fulfilled any of the exclusion criteria, or if they voluntarily withdrew their informed consent. Participation was also discontinued if the participant experienced clinical deterioration, a serious adverse event, poor adherence to the study procedures, or any other condition for which continued participation was considered unsafe or inappropriate by the investigators.